Electrochemical Studies of the Effects of pH and the Surface Structure of Gold Substrates on the Underpotential Deposition of Sulfur

Murat Alanyalıoğlu, Hilal Çakal, A. Emin Öztürk, and Ümit Demir*

Department of Chemistry, Faculty of Arts and Sciences, Atatürk University, Erzurum, Turkey 25240

Received: November 8, 2000; In Final Form: August 29, 2001

The kinetics of the electrochemical deposition and desorption of sulfur monolayers on highly oriented Au(111) and polycrystalline Au electrodes in aqueous solutions containing sodium sulfide was studied by cyclic voltammetry, chronocoulometry, and chronoamperometry. Cyclic voltammetry experiments reveal that underpotential deposition (upd) and stripping of sulfur takes place at two different potentials at polycrystalline Au substrates leading to two oxidative and two reductive peaks. However, sulfur upd consists of only one oxidative and reductive peak at single crystalline Au(111) substrates. Electrosorption valancy measurements and pH dependency showed that the upd of sulfur involved two-electron and one-step mechanism. The charge corresponding to one monolayer of sulfur was determined by cyclic voltammetry and chronocoulometry, indicating a 0.33 coverage. The chronoamperometric results at polycrystalline Au electrodes indicates that deposition takes place in a Langmuir-type mechanism, whereas the stripping of sulfur follows a two-dimensional nucleation and growth mechanism which is accompanied by Langmuir adsorption. Although the appearance of current transients, observed for the deposition of sulfur on Au(111), was similar to what seen for deposition on polycrystalline Au substrates, the stripping process was totally different from deposition, involving only a two-dimensional nucleation and growth mechanism, at pH 12. From an analysis of the desorption current transient, we describe the stripping mechanism as instantaneous. Chronoamperometry experiments suggest that sulfur is first adsorbed on to a Au(111) surface randomly, then reorganizes itself to form a well-ordered structure, and finally strips off in a two-dimensional nucleation and growth mechanism.

Introduction

There has been a great deal of interest in recent years in the growth a thin film compound semiconductors using electrochemical atomic layer epitaxy (ECALE).[1−5] This growth technique takes advantage of the phenomenon of underpotential deposition (upd),[6] where one element deposits onto a second element at potentials more positive than that necessary to deposit the element on itself. The resulting deposit is generally limited to less than a monolayer. Upd has been used to grow binary compound thin film deposits in a layer-by-layer fashion, including CdS,[7−11] ZnS,[12,13] and CdTe.[14,15] It is well-known that upd is strongly affected by the surface orientation of single-crystal electrodes as well as the presence of adsorbing anions in the electrolyte.[16] The upd of sulfur on Au (111) is one of the most intensively investigated by various techniques such as scanning tunneling microscopy (STM),[17] X-ray photoelectron spectroscopy (XPS),[18] modulated reflectance spectroscopy,[19] and surface enhanced raman spectroscopy (SERS).[20] The structure of the initial monolayer formed by upd plays a key role in controlling the structure of subsequently deposited layers; therefore, a great deal of attention has focused on understanding the kinetics of sulfur monolayer deposition. In addition, the knowledge of the behavior of sulfur monolayers on metals is important to understand catalysis, corrosion, and the dynamics of self-assembled monolayers of thiols on metals.

Shannon at al have shown that S monolayers on Au(111) have the $(\sqrt{3} \times \sqrt{3})R30°$ structure, which agrees with observations by Weaver and co-workers.[7] On the basis of coulometric measurements, a total charge of approximately $148 \pm 18\ \mu C/cm^2$ is passed under sulfur upd, which corresponds to a surface coverage of about 0.33 (this is in good agreement with the known coverage of the $(\sqrt{3} \times \sqrt{3})R30° - S$/Au(111) adlattice). Much of the work on the formation of sulfur adlayers at Au-(111) has been done by elucidating the structure and voltammetric behavior of sulfur upd. In a few cases, two sets of peaks have been reported in the upd region. The contrasting results of different authors on the origin of these two peaks is still a matter of debate and complicated, as the voltammetric behavior is pH- and electrolyte-dependent. Arvia et al.[19] have postulated a two-step mechanism involving an initial adsorption of SH^- followed by a two-electron transfer to form an adsorbed S based on the results of in-situ reflectance measurements. Weaver et al.[20] have suggested a similar two-step mechanism by SERS. Both sets of authors have shown no voltammetric data where the second sets of peaks is evident.

The aim of this work is to get further insight into the voltammetric behaviors of sulfur in the upd range. Understanding of this upd process requires better knowledge of the mechanisms of basic phenomena such as the formation of two-dimensional layers of sulfur. An exact interpretation of the atomic surface structure has been observed by STM; however, it requires additional and independent information on the monolayer formation kinetics. A powerful tool for such studies is the chronoamperometric technique since the developments in single crystal substrate preparation have provided new insights in to the processes involved in underpotential deposition. The data obtained from such structurally well-defined substrates suggest that upd is not a simple adsorption processes. One assumption of the Bewick, Fleichman, and Thirsk model

* To whom correspondence should be addressed. Phone: 90 442 2311956. Fax: 90 442 233 1062. E-mail: udemir@atauni.edu.tr.

10.1021/jp004227s CCC: $20.00
Published on Web 10/09/2001

(BFT)[21,22] for nucleation and growth is that the surface is homogeneous and defect free, a high defect density on a surface can have a significant effect on the electrochemical growth mechanism.

Sulfur monolayers have been used to grow binary compounds, including a number of II−IV semiconductors. The efficiency of these materials depends on the single crystalline structure of the semiconductor, in the field of optoelectronics,[23] solar energy conversion,[24] and thin film electroluminescent display.[25] Therefore, the structures of initial sulfur monolayers plays a key role in determining the structure of subsequently deposited layers, as well as the solid-state properties of the films as a whole.

In the present investigation, chronoamperometry, coulometry, and voltammetry techniques were employed to investigate and compare the sulfur upd kinetics on polycrystalline as well as on a carefully prepared single-crystal Au(111) electrodes, under identical electrochemical conditions. An analysis of cyclic voltammograms, obtained at various concentrations and pHs for sulfur upd, suggests that sulfur deposition and stripping processes follow two-electron, one-step mechanism. Current−time transients were analyzed by using two-dimensional nucleation and growth and Langmuirian model for adsorption and desorption. Our results demonstrate that the sulfur is adsorbed randomly on the surface of Au substrates, but it is desorbed in a 2-D nucleation and growth and Langmurian model simultaneously for desorption, depending on the Au substrate structure and pH.

Experimental Section

Preparation of Au(111) Substrates. Au microbead electrodes used in these experiments were prepared as previously described.[11] These polycrystalline electrodes contain some large elliptical (111) facets (visible by eye) with lateral dimensions of approximately 1000 μm. Prior to each experiment, the electrode was flame-annealed for 20 s, and after a short time cooling in air, the electrode was quenched in Milli-Q water. This procedure was repeated five times. Then, the polycrystalline regions were coated with a chemically inert epoxy (Epoxy-Patch), thereby allowing the voltammetric response of the exposed single crystal facets to be measured. These surfaces, because they have not been mechanically polished, possess an extremely low defect density and are ideal for carrying out kinetic studies.

The voltammetric responses of the (111) facets were verified by examining the upd of Cu and Pb at the Au(111) facet electrode. These results are consistent with earlier reports of Cu and Pb upd with respect to the formal potentials, the relative intensities of the voltammetric features, and the width of the upd peaks. All surface area determinations was done by chronoamperometric technique in 5.0 mM $Fe(CN)_6^{3-}$ aqueous solutions containing 1M KCl in according to Cottrell equation for both polycrystalline and single-crystal Au(111) electrode.

Electrochemistry. All electrochemical measurements were carried out in a single-compartment, three-electrode Teflon cell using a BAS 100W electrochemical analyzer. Cyclic voltammetric and chronoamperometric measurements were performed with a solution-handling manifold that allows solutions to be exchange without exposing the electrode to the laboratory ambient and that allows all depositions to be carried out under dry nitrogen gas. In all cases, an Ag/AgCl electrode served as reference electrode, and a platinum wire was used as counter electrode. The electrolyte solution was prepared from ultrapure (Milli-Q) water, $Na_2S{\cdot}9H_2O$ (reagent grade; Aldrich), and appropriate buffer solutions. Before each series of measurements, solutions were deaerated with purified nitrogen prior to addition of Na_2S, to remove dissolved oxygen.

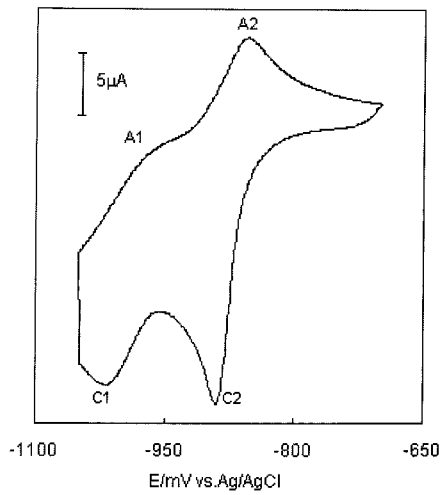

Figure 1. Underpotential deposition of sulfur on polycrystalline Au in 2 mM Na_2S at pH 12. The scan rate was 100 mV/s, and the electrode area was 0.071 cm^2.

Results and Discussion

Sulfur upd on Polycrystalline Substrates. A typical cyclic voltammogram for the upd of sulfur on polycrystalline Au in sulfide solution (pH 12) is shown in Figure 1, at 100 mV/s. It is clearly seen that the deposition takes place at two energetically well-separated waves, shown as peak A1 at about −965 mV and peak A2 at −860 mV. The corresponding dissolution peaks are shown by peaks C1 (−1020 mV) and C2 (−895 mV). Although similar voltammograms on polycrystalline Au substrates were observed in the most of published data, the peaks A2 and C2 have been assigned as upd deposition, but the origin of peaks A1 and C1 has not been discussed in details or not observed by some authors at all. In all of these studies, two possible reasons for the A1/C1 wave have been proposed but no experimental data has been reported to our knowledge.[12] These proposed explanations are as follows. First, the peaks A1/C1 may be dependent upon the identity of the anion in the electrolyte solutions, as well as the presence of halide anions in the electrolyte. It is known that the presence of certain adsorbing anions in the electrolyte can affect the deposition process as well as the structure of electrodeposited layers.[26] Therefore, we intentionally added 0.05 M solutions of Cl^-, CH_3COO^-, NO_3^-, SO_4^{2-}, and PO_4^{3-} anions to determine whether any of these two waves was influenced by the adsorption of these anions. If the A1/C1 wave arises from any of these anions, then cyclic voltammogram will only consist of the A2/C2 wave in the absence of corresponding anion. We found that the A1/C1 wave was always present, When these anions were present, the shape of peaks was affected very little, in terms of sharpness, peak current, and peak potential. Therefore, we can rule out the first proposal that the A1/C1 wave results from coadsorption of anions in the electrolyte solution.

Second, as proposed by White and co-workers, for sulfur upd deposition on Ag(111),[27−29] electro oxidation of HS^- may proceed through a two-step mechanism, and each of these steps leads to a voltammetric wave with a different potential, involving one electron. Briss and Wright[30] also suggested similar two-step mechanism. To determine whether the same mechanism takes place for sulfur adsorption and desorption on Au-

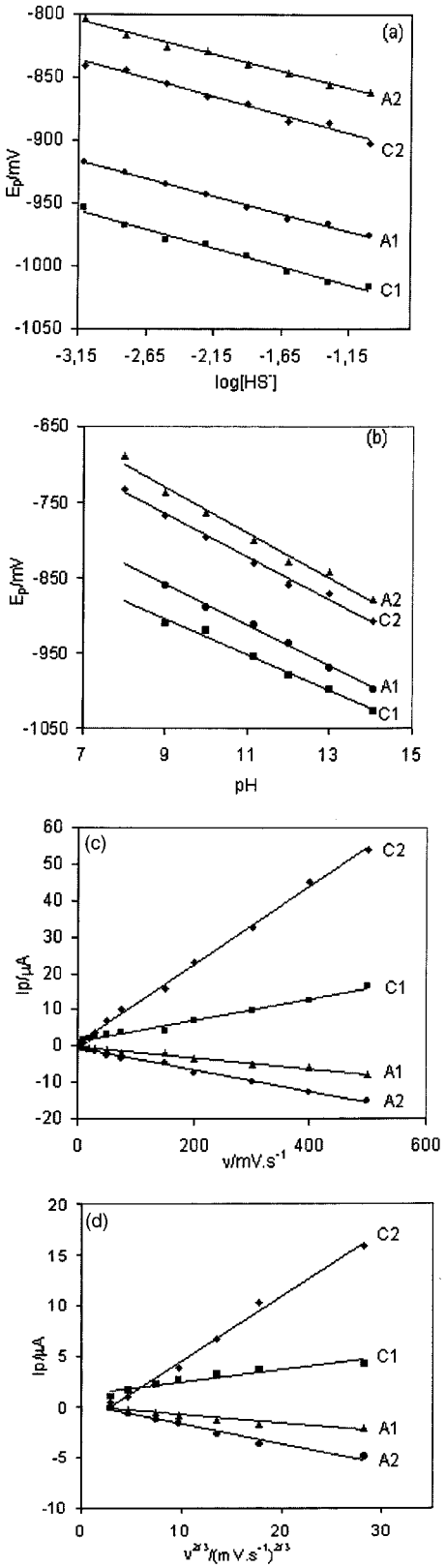

Figure 2. Anodic and cathodic peak potentials for waves A1, A2, C1, and C2 as a function of log HS^- (a) and pH (b) at 100 mV/s scan rates. Scan rate (c) and $^2/_3$ power of the scan rate (d) dependency and of the sulfur underpotential deposition and desorption peak currents.

(111), we measured the dependence of E_p on the concentration of HS^- and pH. As can be seen in Figure 2a, the potentials of A1/C1 and A2/C2 waves are dependent on the concentration of HS^-. The slopes of the E_p versus log [HS^-] plot are about 28 ± 4 mV for each peak, which is in reasonable agreement with the value of 30 mV per decade change in the concentration of HS^- anticipated for two electrons. Moreover, Figure 2b shows a plot of E_p versus pH for the same peaks. The slopes (29 ± 3mV) are also very close to the anticipated value of 30 mV per pH unit for a one proton per two-electron redox process.

The coulometric charge associated with the peak A1 and A2, obtained by chronocoulometry and integration of the area of under these two anodic deposition peaks in Figure 1, gave a value of 150 ± 10 $\mu C/cm^2$ after subtracting from the capacitive charging contribution. This result agrees well with that obtained for the $(\sqrt{3} \times \sqrt{3})R30°$ sulfur structure. Integration of the area under wave A2 alone yields a charge of 110 ± 10 $\mu C/cm^2$, which is not enough to account for the 0.33 coverage, that found for sulfur monolayer. We found that different amounts of charge are consumed during the A1 and A2, and the charge ratio (QA1/QA2) was dependent to the concentration, pH, and the scan rate, but in all cases, the total charge for both peaks was around 150 ± 10 $\mu C/cm^2$. All of these results suggest that the voltammetric waves involve a two-electron transfer as shown by the following equation:

$$(SH^-)_{ad} - 2e^- \leftrightarrow S_{ad} + H^+ \qquad (1)$$

where the subscript "ad" refers to an adsorbed species. Weaver and et al.[19] suggested a similar mechanism for sulfur adsorption on gold using SERS, but they reported a single voltammetric wave corresponding A2/C2 at pH 12. We also found that the A1/C1 wave can be seen more clearly in the pH range 10−13. The A1/C1 wave was scarcely observed at pH values less than 10 and more than 13. Because the dominant sulfur species are HS^- at pH 9−12[20] and the A1/C1 could be observed at these pHs, the origin of these peaks can be attributed to adsorption of HS^- at different energetically distinct sites on polycrystalline Au substrates.

Figure 2c shows the dependence of voltammetric response of each wave on scan rate ν. As seen from the figure, the peak currents for all four peaks are proportional to ν and have a linear dependence showing that these four peaks are associated with the surface processes. If the peak currents are plotted as a function of $\nu^{2/3}$, the plots appear nonlinear over the entire range of scan rates we studied. However, plots for C2, A2, and A1 appear linear below 150 mVs^{-1} (Figure 2d). A $\nu^{2/3}$ scan rate dependency of the peak current is characteristic of a two-dimensional nucleation and growth mechanism.[31,32]

Sulfur Upd at Au(111) Single Crystalline Substrates. The voltammetric response of the Au(111) single-crystal electrode in an aqueous solution containing Na_2S at pH 12 is shown in Figure 3. It is interesting to note that we see only the A2/A2 wave for sulfur upd under the same experimental conditions as on polycrystalline Au substrates. An anodic wave (labeled A2) and a cathodic wave (C2), appearing at −865 and −915 mV, correspond to the deposition and striping of sulfur layer. Integration of the anodic and cathodic peaks (A2, C2) leading to the formation of sulfur layer yields a charge 140 ± 10 $\mu C/cm^2$ (approximately the same charge as that for the polycrystalline surface, for two peaks) corresponding to roughly $^1/_3$ coverage with respect to Au atoms per cm^2, provided that two electrons transferred per HS^-. We examined the effect of the pH and the concentration of HS^- on the potential shift for each E_p (Figure 4a,b) and found similar results to that for polycrystalline Au. The slopes of the E_p versus log [HS^-] and pH plot are about 28 ± 2 and 29 ± 3mV, respectively, indicating a two-electron redox process. Moreover, the ΔE_p ($E_{p,C2} - E_{p,A2}$) is about 30 mV at low scan rates, suggesting a reversible two-electron transfer. The peak currents for A2 and C2 are

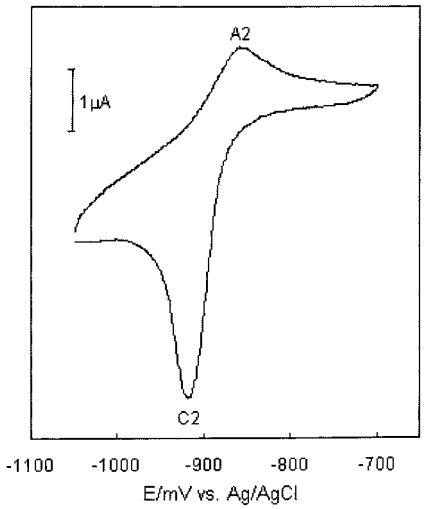

Figure 3. Underpotential deposition of sulfur on single crystalline Au(111). Same electrochemical conditions as described in Figure 1. Electrode area = 0.0105 cm^2.

proportional to ν and have a linear dependence indicating that these peaks are associated with the surface processes (Figure 4c). We also tested all of the anions used on the polycrystalline Au substrate, to see if there was coadsorption or not. We did not observe the A1/C1 wave in any the presence of anion. The question is what causes the A1/C1 wave to appear on the polycrystalline Au but not on the single crystalline Au(111) substrates? More recently, Salvarezza at al[33] have observed very small waves corresponding to A1/C1 on Au(111) prepared by evaporation. They were able to show by STM that these very small peaks are due to adsorption of sulfur atoms at step edges, leading to one-dimensional structures. The upd process of sulfur is quite sensitive to the surface structure of Au substrates. Therefore, we believe that the origin of the differences in the voltammetric behavior of sulfur upd on single- and polycrystalline Au originates from the surface structure of Au substrates.

Chronoamperometry. Chronoamperometry experiments were performed in order to investigate the sulfur nucleation and growth process in more detail. The potential of the working electrode was stepped from an initial value, where no oxidation of sulfide took place, to potentials sufficiently positive to initiate nucleation and growth, after a short induction time. To eliminate double layer charging currents from the transients, the background transient obtained in the absence of Na_2S were taken and subtracted electronically from the those obtained in the presence of Na_2S. Typical current density−time transients for adsorption and desorption of sulfur at Au(111) are presented in Figure 5. The shape of the transients for adsorption exhibit classic Langmuir-type of adsorption.[34] The current density for this adsorption process can be modeled using a simple exponential of the form

$$j_{ads} = k \exp(-k't) \qquad (2)$$

In this process, current density is related to the empty surface area, and sulfur atoms are adsorbed on the Au(111) surface wherever it is empty. Therefore, current starts from a maximum and decays to zero exponentially at about 20 ms, which indicates that diffusion of HS^- from bulk solution is not involved in the growth of sulfur monolayers. Adsorption by this process is considered as a random adsorption. Although it results in a layer formation, the structure of the sulfur layer seems to be not well ordered at the time scale of deposition.

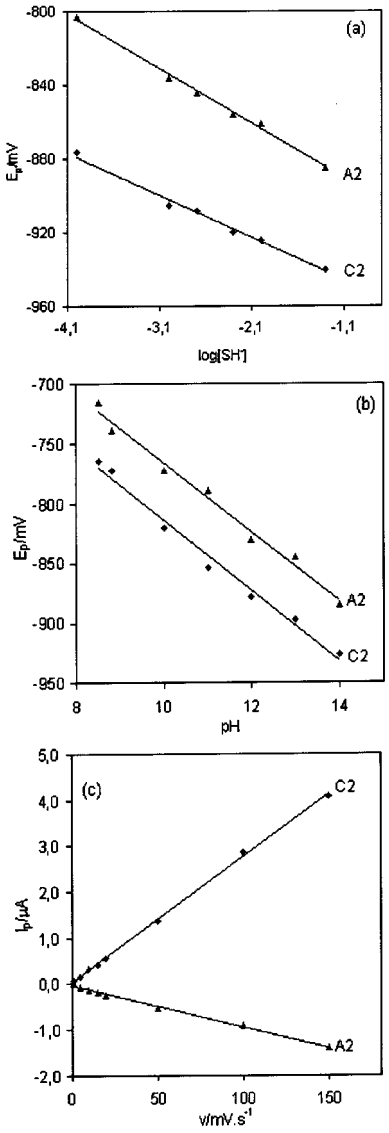

Figure 4. Anodic and cathodic peak potentials for waves A2 and C2 as a function of log HS^- (a) and pH (b) at 100 mV/s scan rates. Scan rate dependency of the sulfur underpotential deposition and desorption peak currents (c).

The appearance of the current density−time transients observed for desorption of the sulfur layer is completely different from what is seen for adsorption. Rising transients are observed for desorption with current maximum at about 15 ms (Figure 5). The current density increases because of the dissolution of the sulfur monolayer. The rising current density eventually reaches a current density maximum, j_m, as the edge area of discrete pits becomes larger. After j_m has been reached, the current decays as the edge area of these pits become smaller. This behavior is major evidence for two-dimensional nucleation and desorption process. Because we observed that a certain amount of time is required to pass in order to see the transient maximum for desorption, after the deposition process, we can conclude that sulfur is adsorbed on to Au(111) surface randomly first then it reorganize itself to form a well ordered structure, then it desorbs in a two-dimensional nucleation process.

A well-established and frequently used model for nucleation and growth is the BFT model.[21,22] Fundamentally, two-dimensional nucleation and growth can be described as either instantaneous or progressive. Although the dissolution sites are activated at the beginning of potential step experiments in the

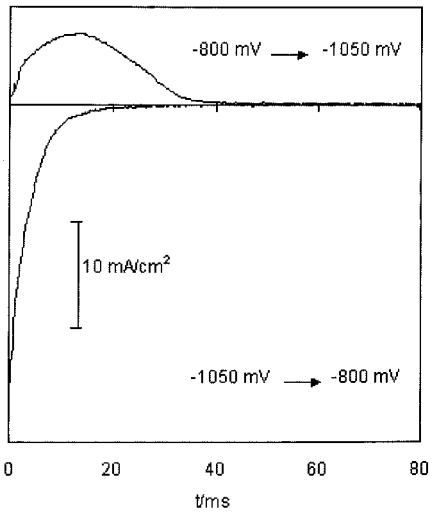

Figure 5. Current−density transients of the cyclic voltammogram (Figure 3) for sulfur upd on single crystalline Au(111). Potential steps are indicated in the figure.

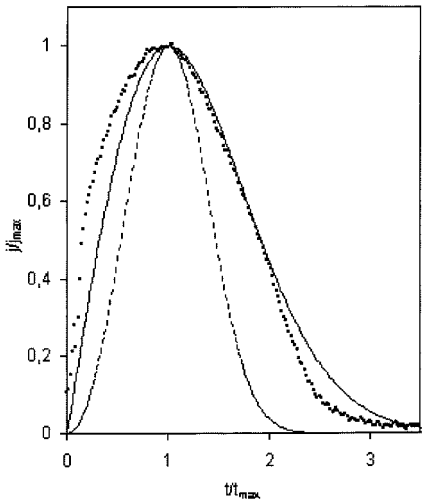

Figure 6. Reduced variable plots for the current−density transient for the peak C2 (···) shown in Figure 5. Values of j/j_{max} are plotted as a function of t/t_{max}. Theoretical curves for instantaneous (—) and progressive (- - -) nucleation are also shown for comparison.

instantaneous model, dissolution sites become activated gradually as the experiment proceeds in the progressive model. The expected current densities for these two cases are

$$j_{ins} = at \exp(-bt^2) \tag{3}$$

for the instantaneous case, and

$$j_{prog} = ct^2 \exp(-dt^3) \tag{4}$$

for the progressive case. A reduced variable plot of the measured quantities (j/j_{max} vs t/t_{max}) allows us to distinguish between these two types of nucleation behavior.[35] Figure 6 shows the reduced variables plots for the desorption transients shown in Figure 5. Calculated transients for instantaneous and progressive nucleation are shown for a direct comparison with the experimental data. The reduced variable plot clearly indicates that the general dissolution mechanism is instantaneous, indicating that the maximum numbers of dissolution sites are activated or present at the beginning of dissolution. This was shown in STM experiments, where the sulfur layers have a large number of pits.[12]

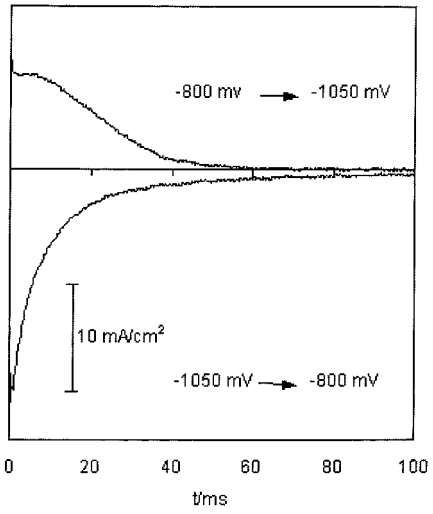

Figure 7. Current−density transients of the cyclic voltammogram (Figure 1) for sulfur upd on polycrystalline Au. Potential steps are indicated in the figure.

Figure 7 shows the current density transients obtained at a polycrystalline Au electrode under the same experimental conditions as those in Figure 5. Although the curves look similar to what has been seen on Au(111) substrates for deposition, the curves for dissolution show a shoulder rather than a current maximum, and the experimental data did not fit either of the above-described models. This behavior has previously been observed for one of the upd peaks in Cu deposition.[36] In this case, random adsorption and 2-D nucleation and growth processes occur simultaneously at different surface site. It is known that surface defects such as monatomic steps, kink sites, holes, etc. are preferred sites for adsorption. The simplest model is to consider the current density as the sum of two independent terms, a Langmuir-type of adsorption−desorption term and a nucleation growth term as shown by the following equation:

$$j_{total} = j_{ads} + j_{nucl/growth} \tag{5}$$

A fit of the measured transient was attempted in order to separate the random desorption from the instantaneous process, with this equation using least-squares fits and working with multidimensional Newton routines. Figure 8 shows excellent fit of the data obtained for the random desorption and instantaneous desorption process that take place simultaneously. The individual current contributions of the random desorption and the instantaneous process to the total current can be obtained from this numerical fit. Figure 8 also shows that 65% of the total current is due to the random and 35% is due to the instantaneous desorption process. This ratio of random desorption to 2-D desorption is dependent on the surface morphology of the polycrystalline substrate, indicating that random desorption starts at surface defects. These conclusions lead us to think that it is possible to get more ordered sulfur monolayers on a single crystalline Au(111) substrate than on a polycrystalline Au substrate.

Effects of pH on Current Transients at Au(111). Figure 9 shows the influence of the pH on the current transients at single crystalline Au(111) substrates for the peak C2. All of these transients were taken under the same electrochemical conditions except for the pH. Transients were subtracted from the transients taken at blank solutions. The shape of the transients at pH 14 reveals that random and two-dimensional desorption take place in parallel. When the pH drops, the charge for random dissolution gets smaller, but the charge for dissolution with 2-D nucleation and growth increases. At pH's 12 and 10, the current

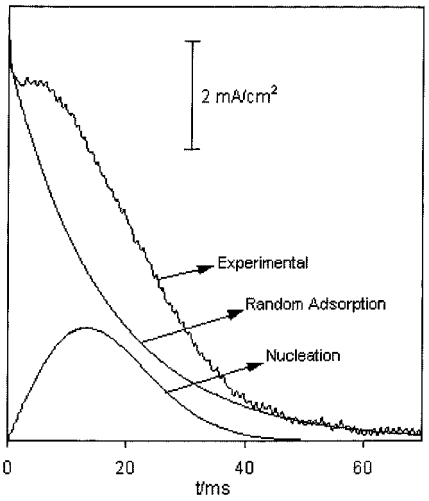

Figure 8. Numerical fit of the random adsorption−nucleation model (eq 4) to a transient for the desorption peak of sulfur underpotential (C2). The individual contributions of adsorption and nucleation are also shown.

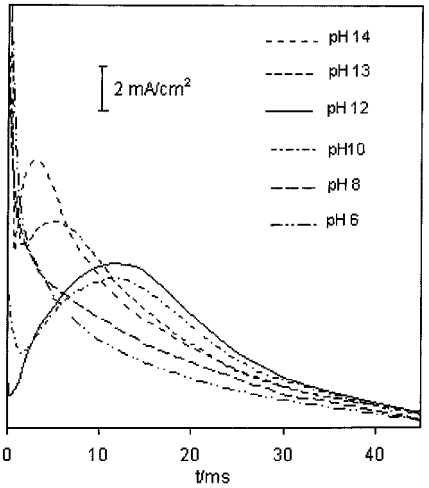

Figure 9. Dependency of current−density transients for the underpotential desorption (C2) of sulfur on pH at Au(111). The potential step is from −800 to −1050 mV.

transients have no random desorption component and consist of only two-dimensional desorption. The current transients starts to have a random desorption component at pH's less than 10, and it increases with the decrease of pH. Finally, the transients recorded for pH 8 have no charge corresponding to the two-dimensional nucleation and growth process at all. As shown in Figure 9, these current density transients exhibit the classic shape of nucleation process; after the decay of a sharp electrode double layer charging current, the current increases because of nucleation and growth of sulfur nuclei and reaches to a maximum. When the pH decreases maximum shifts to longer times. After pH 10, no maximum is observed. When pH increases, the nucleation density increases, and this shortens the time required for the sulfur monolayer completion. These current maximum shifts are similar to those obtained when the overpotential increases.[22,36] The pH dependences of these transients can be explained by taking into account that the concentration of sulfur species (H_2S, HS^-, and S^{2-}) depends on the solution pH. Therefore, HS^- is the only significant species at pH 9−12. The fact that we do not observe two sets of peaks at Au(111), as seen for polycrystalline Au, and that dissolution of sulfur takes place in a two-dimensional nucleation and growth process at pH 10−12 leads us to conclude that HS^- forms more ordered sulfur monolayers than the other sulfur species.

Conclusions

We have studied the influence of pH and the substrate structure on the kinetics of sulfur adsorption and desorption. We found that the underpotential deposition and desorption of sulfur takes place at two different potentials with two sets of peaks at polycrystalline Au substrates, whereas there is only one set of peaks for single crystalline Au substrates indicating that there are two possible adsorption sites for HS^- at polycrystalline Au electrodes. HS^- concentration and pH dependency experiments revealed that upd of sulfur involves a two-electron one-step mechanism for each peak. Our chronoamperometric results suggest that the deposition follows a Langmuir-type mechanism, whereas the dissolution of sulfur takes place in a nucleation and growth process, with both preceding at different electrode sites depending on pH at Au(111).

References and Notes

(1) Gregory, B. W.; Stickney, J. L. *J. Electroanal. Chem.* **1991**, *300*, 543.
(2) Villegas, I.; Stickney, J. L. *J. Electrochem. Soc*. **1992**, *139*, 686.
(3) Suggs, D. W.; Stickney, J. L. *Surf. Sci*. **1993**, *290*, 362.
(4) Colletti, L. P.; Teklay, D.; Stickney, J. L. *J. Electroanal. Chem.* **1994**, *369*, 145.
(5) Stickney, J. L. In *Electroanalytical Chemistry*; Bard, A. J., Rubinstein, I., Eds.; Marcel Dekker: New York, 1999; Vol. 21, p 75.
(6) Kolb, D. M. In *Advances in Electrochemistry and Electrochemical Engineering*; Gerischer, H., Tobias, C. W., Eds.; Wiley Interscience: New York, 1978; Vol. 11, p 125.
(7) Demir, U.; Shannon, C. *Langmuir* **1994**, *10*, 2794.
(8) Demir, U.; Shannon, C. *Langmuir* **1996**, *12*, 594.
(9) Gichuhi, A.; Boone, B. E.; Demir, U.; Shannon, C. *J. Phys. Chem. B* **1998**, *102*, 6499.
(10) Guidelli, R.; Innocenti, M.; Aloisi, G.; Cavallini, M.; Pezzatini, G. G.; Foresti, L. M. *J. Phys. Chem. B* **1998**, *102*, 7413.
(11) Demir, U.; Shannon, C. *Langmuir* **1996**, *12*, 6091.
(12) Gichuhi, A.; Shannon, C.; Perry, S. S. *Langmuir* **1999**, *15*, 5654.
(13) Torimoto, T.; Obayashi, A.; Kuwabata, S.; Yasuda, H.; Mori, H.; Yoneyama, H. *Langmuir* **2000**, *16*, 5820.
(14) Huang, B. M.; Coletti, L. P.; Gregory, B. W.; Anderson, J. L.; Stickney, J. L. *J. Electrochem. Soc*. **1995**, *142*, 3007.
(15) Coletti, L. P.; Flowers, B. H., Jr.; Stickney, J. L. *J. Electrochem. Soc*. **1998**, *145*, 1442.
(16) Aramata, A.; Taguchi, S. *J. Electroanal. Chem.* **1998**, *457*, 73.
(17) Gao, X.; Zhang, Y.; Weaver, M. J. *J. Phys. Chem.* **1992**, *96*, 4156.
(18) Buckly, A. N.; Hamilton, I. C.; Woods, R. *J. Electroanal. Chem.* **1987**, *216*, 213.
(19) Lezna, R. O.; Arvia, J. A.; de Tacconi, N. R. *J. Electroanal. Chem.* **1990**, *283*, 319.
(20) Gao, X.; Zhang, Y.; Weaver, M. J. *Langmuir* **1992**, *8*, 668.
(21) Bewick, A.; Fleiscmann, M.; Thirsk, H. R. *Trans. Faraday Soc.* **1962**, *58*, 2200.
(22) Fleiscmann, M.; Thirsk, H. R. In *Advances in Electrochemistry and Electrochemical Engineering*; Delahay, P., Tobias, C. W., Eds.; Wiley: New York, 1963; Vol. 3.
(23) Gebhard, W. *Mater. Sci. Eng*. **1992**, *B11*, 1.
(24) Licht, S.; Forouzan, F.; Longo, K. *Anal. Chem.* **1990**, *62*, 1356.
(25) Bhargava, R. N. *J. Cryst. Growth* **1982**, *59*, 15.
(26) Michaelis, R.; Zei, M. S.; Zhai, R. S.; Kolb, D. M. *J. Electranal. Chem.* **1992**, *339*, 299.
(27) Hatchett, D. W.; White, H. S. *J. Phys. Chem.* **1996**, *100*, 9854.
(28) Hatchett, D. W.; Gao, X.; Catron, S. W.; White, H. S. *J. Phys. Chem.* **1996**, *100*, 331.
(29) Conyers, J. L., Jr.; White, H. S. *J. Phys. Chem. B* **1999**, *103*, 1960.
(30) Birss, V. I.; Wright, G. A. *Electrochim. Acta* **1982**, *27*, 1.
(31) Sanchez-Maestre, M.; Rodriguez-Amaro, R.; Munoz, E.; Ruiz, J. J.; Camacho, L. *J. Electroanal. Chem.* **1994**, *373*, 31.
(32) Bosco, E.; Rangarajan, S. K. *J. Electroanal. Chem.* **1981**, *129*.
(33) Vericat, C.; Andreasen, G.; Vela, M. E.; Salvarezza, R. C. *J. Phys. Chem. B* **2000**, *104*, 302.
(34) Barradas, R. G.; Bosco, E. *J. Electroanal. Chem.* **1985**, *193*, 23.
(35) Harrison, J. A.; Thirsk, H. R. In *Electroanalytical Chemistry*; Bard, A. J., Ed.; Marcel Dekker: New York, 1971; Vol. 5.
(36) Hölzle, M. H.; Retter, U.; Kolb, D. M. *J. Electranal. Chem.* **1994**, *371*, 101.